

**OIL-FROM-WATER REMOVAL UNDER LOW
GRADIENT MAGNETIC SEPARATION (LGMS)**

MUHAIMIN HAZMI BIN KHAI RUNNIZAM

UNIVERSITI SAINS MALAYSIA

2022

OIL-FROM-WATER REMOVAL UNDER LOW GRADIENT MAGNETIC SEPARATION (LGMS)

by

MUHAIMIN HAZMI BIN KHAI RUNNIZAM

**Thesis submitted in fulfilment of the requirement
for degree of
Bachelor's degree in Chemical Engineering**

June 2022

ACKNOWLEDGEMENT

First and foremost, I would like to express my gratitude to Allah SWT for granting me the strength and willpower I require to finish this thesis for my Final Year Project. Without his help, I do not believe I would have been able to complete it. Then, I would like to express my utmost gratitude to my supervisor, Professor Dr Lim Jit Kang, and his post-graduate student, Mr Wei Ming Ng, for their assistance in guiding me through the process of completing this report using their knowledge and experience. I had amassed considerable knowledge in nanoparticles, magnetophoresis, and Pickering emulsions. I am incredibly grateful to both of you.

In addition, I would like to take this opportunity to extend my appreciation to my parents for the love, care, and encouragement they have shown me throughout my entire life. Special thanks go out to my course mates, and lab mates, particularly James, who assisted me in conducting experiments and analyzing the results as most of ours lined up.

Special thanks to the School of Chemical Engineering, USM, for providing me with the funding and the permission to use the nanoparticle laboratory for my experiments. Last but not least, the MARA scholarship for its financial support is greatly acknowledged.

Muhaimin Hazmi Bin Khai Runnizam,

June 2021

TABLE OF CONTENTS

ACKNOWLEDGEMENT	i
TABLE OF CONTENTS	ii
LIST OF TABLES	iv
LIST OF FIGURES	v
LIST OF SYMBOLS	viii
LIST OF ABBREVIATIONS	ix
ABSTRAK	x
ABSTRACT	xi
CHAPTER 1 INTRODUCTION	1
1.1 Magnetic Pickering Emulsions	1
1.2 Problem Statement	3
1.3 Research Objectives	4
1.4 Scope of Thesis	5
CHAPTER 2 LITERATURE REVIEW	6
2.1 Pickering emulsion	6
2.1.1 Pickering emulsion stabilisation	7
2.1.2 Stimuli-responsive and potential application of Pickering emulsion	9
2.2 Iron oxide nanoparticles (IONP)	11
2.2.1 Stabilisation and surface functionalisation of naked IONP	12
2.2.2 IONP and IONP-composites colloidal stability	15
2.3 Magnetic separation	17
CHAPTER 3 METHODOLOGY	23
3.1 Materials	23
3.2 Research flow	23
3.3 Functionalization of IONP	24

3.3.1	Post-coating of IONP with PSS	25
3.4	MPE formation by IONP-PSS and PDDA	26
3.5	Chemical and physical properties of naked IONP, composite of IONP and MPE.	26
3.5.1	Surface properties of naked IONP, IONP-composites and MPE through Zeta-potential	27
3.5.2	Naked IONP, IONP-composites and MPE size measurements	27
3.6	Macroscopic study on MPE colloidal stability and MPE physical motion under LGMS	28
3.7	Oil-to-water Ratio Determination and oil-to-water calibration for LGMS system	29
3.8	Magnetic flux density gradient (dB/dz), ∇B	30
3.9	Image analysis via ImageJ	30
	CHAPTER 4 RESULTS AND DISCUSSION	32
4.1	Surface analysis for naked IONPs, IONP-PSS, IONP-PSS-PDDA and MPE through Zeta-potential	32
4.2	Size analysis of naked IONPs, IONPs-composites and MPE through DLS	39
4.3	Macroscopic scale analysis of MPE colloidal stability and MPE motion under LGMS	42
4.3.1	Without a low gradient magnetic field (colloidal stability of MPE)	43
4.3.2	With low gradient magnetic field (magnetophoresis)	47
4.4	Sustainability	50
	CHAPTER 5 CONCLUSION AND RECOMMENDATIONS	53
5.1	Conclusions	53
5.2	Recommendations	54
	REFERENCES	56
	APPENDICES	66

LIST OF TABLES

	Page
Table 3.1: Materials used, supplier and purpose	24
Table B.2: Grayscale values and normalized volume fraction of dispersed oil for the macroscopic motion of MPE	67
Table B.3: DLS results for zeta potential surface analysis of IONP, IONP-PSS, IONP- PSS-PDDA and MPE.....	70
Table B.4: DLS results for size analysis of IONP, IONP-PSS, IONP-PSS-PDDA and MPE	71

LIST OF FIGURES

	Page
Figure 1.1: Number of tanker oil spills and oil spillage worldwide from 1970 to 2017 (Chen et al., 2019).	1
Figure 1.2: Sketch of a Pickering emulsion and a classical (surfactant-based) emulsion. The solid particles adsorbed at the oil-water interface stabilise the droplets in place of the surfactant molecules (Chevalier and Bolzinger, 2013).....	3
Figure 2.1: The relationship between particle surface contact angle and emulsion structure (Ye et al., 2015).	6
Figure 2.2: Schematic diagrams represent the different destabilisation mechanisms of O/W emulsion (Gupta et al., 2016).	8
Figure 2.3: Stabilisation strategies reviewed for the naked IONP (Tham <i>et al.</i> , 2021)..	12
Figure 2.4: Illustration shows a layer-by-layer polyelectrolyte approach where adsorption of charged materials to oppositely charged surfaces (McShane and Lvov, 2014).....	14
Figure 2.5: Illustration of the evolution of the micelle-like structure of surfactants on polyelectrolyte as surfactant concentration increases (Khan and Brettmann, 2018).....	15
Figure 2.6: HGMS and LGMS processes (Leong et al., 2016a).....	18
Figure 3.1: Flow diagram on a research project for oil-from-water removal under LGMS.	23
Figure 3.2: Macroscopic motion for MPE magnetophoresis under LGMS by real-time image capturing via camera.	29
Figure 4.1: The zeta-potential profile of naked IONPs, IONP-PSS, IONP-PSS-PDDA and MPE at different pHs of suspensions.	33

Figure 4.2: Schematic diagram of the surface of IONP-PSS-PDDA at acidic and alkaline pH (Che et al., 2014; Tham et al., 2021).	37
Figure 4.3: The emulsion droplet surfaces are stabilized by the synergism of IONP-PSS-PDDA and adjacent PDDA molecules at certain pH values (Che et al., 2014; Tham et al., 2021).....	38
Figure 4.4: The average hydrodynamic diameter profile of naked IONPs, IONP-PSS, IONP-PSS-PDDA and MPE.....	40
Figure 4.5: Nanoparticles interaction of IONP-PSS-PDDA at acidic pH and alkaline pH.	41
Figure 4.6: Mean grayscale value with respect to the volume fraction of dispersed oil according to the oil-water ratio used in MPE.....	43
Figure 4.7: Three sequence of time-lapse images showing the turbidity changes of MPE over two hours due to the flocculation of MPE. The MPE was dispersed in a solution with (a) pH 3, (b) deionized water and (c) pH 10.....	44
Figure 4.8: Time-dependent normalized volume fraction dispersed oil profiles of MPE over 120 minutes (2 hours) in deionized water, pH 3 (acidic) and pH 10 (alkaline).....	45
Figure 4.9: Time-dependent normalized volume fraction dispersed oil profiles of MPE over 30 minutes in deionized water, pH 3 (acidic) and pH 10 (alkaline)..	45
Figure 4.10: Photo series for magnetophoresis of MPE under LGMS at (a) pH 3, (b) deionized water and (c) pH 10.....	47
Figure 4.11: MPE magnetophoresis profile time-dependent normalized volume fraction graph under three conditions (deionized water, pH 3 and pH 10) over 120 minutes (2 hours).....	48

Figure 4.12: MPE magnetophoresis profile time-dependent normalized volume fraction graph under three conditions (deionized water, pH 3 and pH 10) over 30 minutes (1800 seconds).	49
Figure A.1: UV scan of naked IONPs, IONP-PSS, PSS and PDDA.....	66

LIST OF SYMBOLS

Symbol	Description	Unit
B	Magnetic flux density/magnetic field	T/m
B_r	Remanence flux density	G
∇B	Magnetic flux density gradient/magnetic field gradient (dB/dz)	T/m
D_t	Diffusion coefficient	-
d_h	Hydrodynamic diameter	nm
η	Viscosity	Pa.s
F_{drag}	Viscous drag force	-
F_{mag}	Magnetophoretic force	-
ΔG_d	Free energy of desorption	-
H_m	Magnetic field strength/ magnetic field	
H_{cm}	Height of cylindrical magnet	mm
k_B	Boltzmann constant	-
M_r	Remanent Magnetization	emu/g
m_p	Total mass of IONPs	g
R_m	Radius of cylindrical magnet	mm
r	Hydrodynamic radius	nm
θ	Contact angle	°
z	Distance from magnet	cm

Greek letter

μ	Magnetic dipole moment
-------	------------------------

LIST OF ABBREVIATIONS

CMC	Critical micelle micellization
DLS	Dynamic light scattering
FTIR	Fourier transform infrared spectroscopy
HGMS	High gradient magnetic separation
IONP	Iron oxide Nanoparticle
IONP-PSS	Poly (sodium 4-styrenesulfonate) coated iron oxide nanoparticle
IONP-PSS-PDDA	Poly (diallyldimethylammonium chloride) and poly (sodium 4-styrenesulfonate) coated iron oxide nanoparticle
LGMS	Low gradient magnetic separation
MPE	Magnetic Pickering emulsion
O/W	Oil-in-water
PSS	Poly (sodium 4-styrenesulfonate)
TEM	Transmission electron microscopy
W/O	Water in oil
UV-Vis	Ultraviolet-visible light

**PENYINGKIRAN MINYAK-DARIPADA-AIR DI BAWAH PEMISAHAN
MAGNETIK KECERUNAN RENDAH (LGMS)**

ABSTRAK

Emulsi Pickering Magnet (MPE) yang mempunyai responsif magnetik telah distabilkan oleh nanozarah besi oksida (IONP) di salut dengan poli(natrium 4-stiresulfonat) dan poli(dialildimetilammonium klorida) (PDDA) serta molekul PDDA bersebelahan. MPE, IONP, IONP-PSS dan IONP-PSS-CTAB disintesis and dikajikan dengan siri pencirian bagi kelakuan kimia, fizikal dan magnetik. Dalam kajian makroskopik, imej bagi ubah kekeruhan MPE dirakamkan oleh kamera telefon pintar dengan intervalometer. ImageJ telah digunakan untuk menganalisa semua imej. Pada skala makroskopik, pemisahan magnetik untuk MPE telah mencapai keberkesanan 80% dalam masa 30 minit bagi semua keadaan. Walaubagaimanapun, kestabilan berkolid bagi MPE dalam pH 10 adalah paling rendah berbanding dengan keadaan pH 3 dan air ternyaion di bawah jangka masa flokulasi 2 jam. MPE dalam pH 10 memerlukan jangka masa yang singkat untuk mencapai keefisienan pemisahan yang tertinggi. Oleh sebab itu, MPE dalam pH 10 mengalami magnetoforesis secara berkerjasama apabila pengelompokan tidak berbalik terdapat dalam MPE semasa magnetoforesis. Ketika kajian makroskopik, MPE tidak mengalami pemecahan bawah medan magnetik, B dengan nilai 0.02 T ~ 0.64 T dan kecerunan medan magnetic (dB/dz), ∇B dengan nilai 25.09 T/m ~ 94.57 T/m. Magnetoforesis juga menunjukkan liputan permukaan bagi MPE bersesuaian dengan potensi zeta MPE yang positif tinggi. Hal ini kerana selain IONP-PSS-PDDA, molekul PDDA meliputi bilangan yang tinggi pada permukaan titisan-titisan emulsi.

OIL-FROM-WATER REMOVAL UNDER LOW GRADIENT MAGNETIC SEPARATION (LGMS)

ABSTRACT

A magnetic Pickering emulsion (MPE) was synergistically stabilized by the iron oxide nanoparticles (IONPs) coated by poly(sodium 4-styrenesulfonate) (PSS) and poly(diallyldimethylammonium chloride) (PDDA) as well as the adjacent PDDA molecules. MPE, IONP, IONP-PSS, and IONP-PSS-PDDA were synthesised. Their chemical, physical, and magnetic characteristics were analysed in depth. Under macroscopic motion of MPE, the synthesised MPE was examined. A smartphone camera captured the fluctuating turbidity of the MPE suspension. ImageJ was used to analyse all photos. The MPE magnetic separation efficiency reached 80% in 30 minutes on a macroscopic scale under all conditions. However, the MPE colloidal stability was lowest at pH 10 compared to pH 3 and DI water under a flocculation time of 2 hours. MPE at pH 10 needed the least time to achieve the greatest separation efficiency. As a result, MPE at pH 10 exhibited cooperative magnetophoresis, as it irreversibly flocculated during magnetophoresis. During the macroscopic study, the MPE did not deform or coalesce under the magnetic field B of 0.02 T ~ 0.64 T and magnetic field gradient (dB/dz), ∇B of 25.09 T/m ~ 94.57 T/m. Magnetophoresis study demonstrated that IONP-composites on emulsion droplets corresponded with significant positive MPE zeta potential. This is because, in addition to IONP-PSS-PDDA, PDDA molecules occupied considerable portions of emulsion droplet surfaces. Magnetophoresis of newly synthesised MPE improved oil recovery prospects.

CHAPTER 1

INTRODUCTION

1.1 Magnetic Pickering Emulsions

The release of petroleum and other oil forms through industrial waste, ships, and unintentional oil spills is detrimental to marine and aquatic ecosystems (Mirshahghassemi and Lead, 2015). For example, an estimated 90 million gallons of oil were discharged into the Atlantic Ocean by the sinking of the Atlantic Empress 16 kilometers off the coast of Trinidad & Tobago (Wells, 2017). The Atlantic Empress and Aegean Captain collided during a tropical storm on July 19, 1979, resulting in the greatest tanker spill in history. These oily discharges create substantial economic losses and harm coastal and other ecosystems. Oil waste can result in habitat loss, direct ecotoxicity, and health issues for local populations (Mirshahghassemi and Lead, 2015).

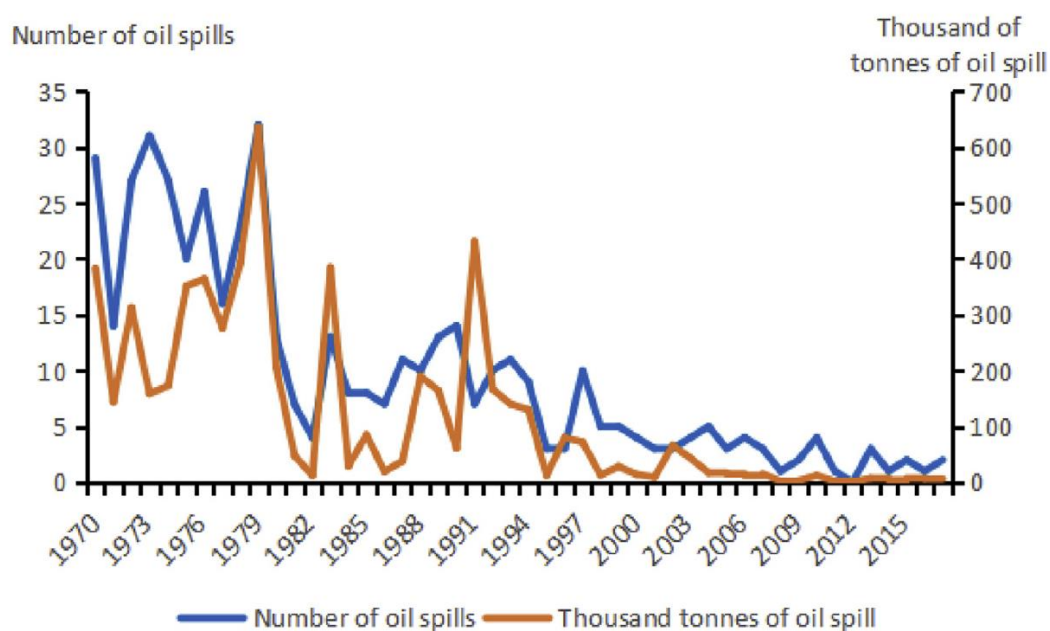


Figure 1.1: Number of tanker oil spills and oil spillage worldwide from 1970 to 2017 (Chen *et al.*, 2019).

There are several methods to recover oil spills, each with varying effectiveness. Booms, for example, necessitate costly and time-consuming cleaning, have disposal

concerns and are incapable of preventing recovered oil from sinking (Chen *et al.*, 2019). Skimming systems are very reliant on sea conditions. In moderately choppy or violent water, skimmers often recover more water than oil (Broje and Keller, 2006). Dispersants are especially harmful to corals, prompting experts to advocate for a ban on dispersant usage near coral reefs (Prince, 2015).

Furthermore, oil-water separator technology is the most commonly used onboard approach for separating oil from ship wastewater discharges. However, substantial onboard space and additional costly post-treatment are required to reach the discharge restrictions. New solutions are actively explored due to the limitations of existing technologies for extracting oil from oil spills and oily discharges. Nanotechnological applications offer a potential research path (Deng *et al.*, 2013; Tratnyek and Johnson, 2006) - specifically, magnetic Pickering emulsions (MNP).

Oil removal through stimuli-responsive Pickering emulsions has attracted significant attention in recent years as an effective tool for pollutant removal from an aqueous environment. Among these are MNP due to its fast response toward an externally applied magnetic field (Tham *et al.*, 2021). The essential premise of this separation procedure is relatively simple. It is due to magnetic materials exhibiting magnetophoretic force under magnetic field gradients, allowing them to be physically isolated from the surrounding fluids by a magnetic source (Lim *et al.*, 2014a). Pickering emulsions have numerous advantages over organic surfactant-stabilised emulsions, including low toxicity, cheap cost, irreversible adsorption, self-assembly capabilities, and enhanced stability (Lin *et al.*, 2015). The figure below shows the basic principle of magnetic Pickering emulsions.

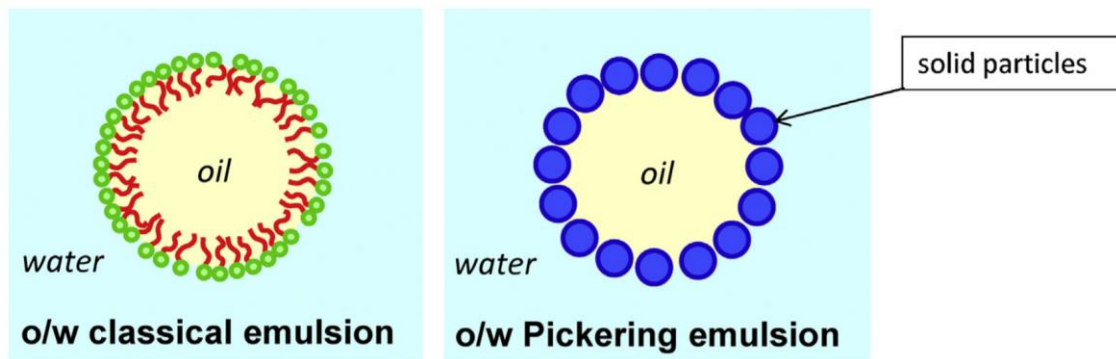


Figure 1.2: Sketch of a Pickering emulsion and a classical (surfactant-based) emulsion. The solid particles adsorbed at the oil-water interface stabilise the droplets in place of the surfactant molecules (Chevalier and Bolzinger, 2013).

1.2 Problem Statement

Water scarcity is a global issue that must be addressed to ensure sustainable access to high-quality water resources. Oily wastewaters discharged by the petrochemical, pharmaceutical, polymer, metal, cosmetic, textile, and food sectors have long constituted a severe environmental and health risk. Produced water, used in gas and oil production, is frequently contaminated with oil, posing serious problems for water resource management. This situation is deteriorating in the Gulf Cooperation Council (GCC) countries, which only have a 1:6 water to the population; hence they rely on wastewater for their water source (Ewis *et al.*, 2020).

Removing oil from water is critical for meeting government-mandated discharge limits. Because of the nature of the oil-to-water composition, the formation of oil-in-water emulsion (or microemulsion) has greatly hampered the design of an effective separation system because these entities are small in size and have a density that is lower than that of water, causing them to float on the water-air interface. Hence, the Pickering

emulsion process could be used to solve the issue. It utilises nanoparticle fluid as a solid emulsifier.

The magnetic responsiveness of the Pickering emulsion is achieved by forming MPE through the adsorption of magnetic nanoparticles to separate the Pickering emulsion. However, the stability of MPE is lower as the variation of the magnetic field is from weak to strong (Melle *et al.*, 2005). Low gradient magnetic separation (LGMS) will be used to modify and separate the MPE without breaking and coalescence. However, just a few published studies could destabilise emulsion droplets with an LGMS.

Numerous studies have used nanoparticles and surfactant combinations of nanoparticles and polymer to create a synergistic effect for stabilising Pickering emulsion. Tham *et al.* conducted a magnetophoresis of MPE using IONP-polymer-surfactant IONP-PSS-CTAB (2021). Most investigations that focus on the macroscopic separation of MPE lack kinetic analysis (Bin *et al.*, 2015; Choi *et al.*, 2018). Therefore, it demands the temporal motion of MPE.

This research investigates a complicated ternary system made up of (i) nanoparticles, (ii) polyelectrolytes, and (iii) surfactants for oil-water emulsion separation. It is hoped that a well-rounded LGMS technology capable of separating a wide range of oily wastewaters may be developed by fine-tuning the ratio of these three components concerning the oil-to-water ratio.

1.3 Research Objectives

1. To develop a magnetic nanoparticle-polyelectrolyte-polyelectrolyte colloidal system for removing oil from aqueous environments.
2. Record the macroscopic separation kinetic profile of an oil-in-water emulsion separation process influenced by a low gradient magnetic field.

3. To determine the oil-to-water ratio range in which the LGMS system may be used as an oily wastewater clean-up approach.

1.4 Scope of Thesis

This thesis focuses on the influences of an externally applied magnetic field on the magnetophoretic collection kinetics of MPE. IONP is used alongside emulsions as it possesses magnetic properties. Hence, the first step of the work was to increase IONP stability. IONP was coated with PSS and PDDA via post coating technique to form IONP-PSS-PDDA. MPE is created when IONP-PSS-PDDA is used to adsorb on the emulsion of dodecane.

A macroscopic study was done to study the colloidal stability of the emulsion. It is mainly affected by: pH, temperature, ionic strength, and emulsion size (Pang *et al.*, 2012). The pH conditions of the solution significantly influenced MPE's macroscopic motion. The pH might impact the surfactant-polymer interaction (Petkova *et al.*, 2013). The size measurements and magnetic characteristics were used to characterise them. The pH suspensions could influence the zeta potentials of IONP, IONP composite, and MPE. The PSS and PDDA layers have negative and positive charge groups, respectively. Consequently, a series of measurements of the zeta potential of IONP, IONP-composites, and MPE were performed throughout a pH range of 3 to 10. In addition, the influence of pH on the dimensions of IONP-composites and MPE will be investigated.

MPE was created in a cuvette for the macroscopic motion after being diluted 50 times. The transport processes of MPE with the presence of LGMS (magnetophoresis) and the absence of LGMS (creaming) were captured in real-time by a camera. The macroscopic mobility of MPE was also investigated at pH 3, pH 10, and DI water. The kinetic profiles of these two processes were then plotted and studied.

CHAPTER 2

LITERATURE REVIEW

2.1 Pickering emulsion

The most significant distinction between a Pickering emulsion and a classical emulsion is that the former contains solid particles at the interface between two liquid phases that serve as the stabilising agent, whilst the latter relies on molecular surfactants to stabilise emulsions (Pickering, 1907). There are two main types of Pickering emulsions: oil-in-water emulsions (O/W) and water-in-oil emulsions (W/O). The type is defined by the solid particle's contact angle at the water and oil interface, as illustrated in Figure 2.1.

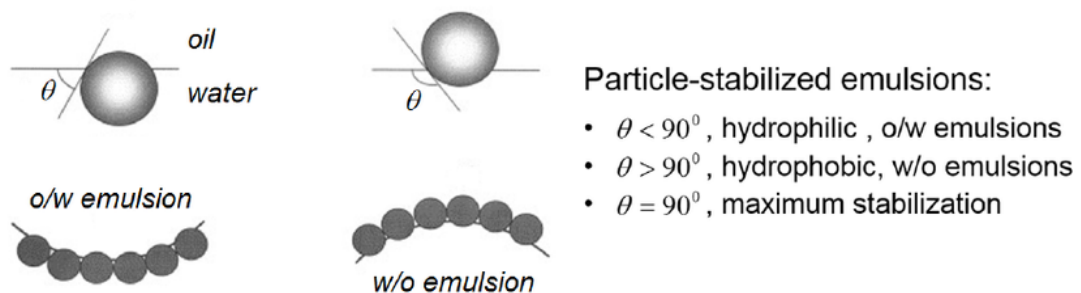


Figure 2.1: The relationship between particle surface contact angle and emulsion structure (Ye *et al.*, 2015).

Nanoparticles (NPs) with a contact angle at the oil-water interface less than 90° are hydrophilic, stabilise O/W, and will curve towards the water phase. Whereas those with a contact angle over 90° are hydrophobic, produce W/O emulsions, and curve towards the oil phase. Other variables, such as oil type, salinity, and the initial phase volume ratio, determine the type of emulsion created with NPs having a contact angle of approximately 90° .

This high emulsion stability is due to the significant solid particle adsorption under conditions of partial wetness. In brief, the free energy of adsorption (ΔG) of a tiny spherical particle at O/W in Figure 2.1 is calculated as follows:

$$\Delta G = -\pi R^2 \gamma (1 \pm \cos \theta)^2 \quad (2.1)$$

R is the particle radius, γ is the oil-water interface surface tension, and θ is the contact angle determined via the water phase (Aveyard *et al.*, 2003). The energy required to remove a single particle from the interface ($-\Delta G$) is significantly greater than its thermo-energy, indicating it will remain at the interface as long as θ is near 90° (Aveyard *et al.*, 2003). It is valid regardless of nanometer or micrometer range.

The stabilising particles must be adsorbed firmly to produce a Pickering emulsion. Some studies have shown that emulsifiers with weakly aggregated particles with diameters in nanometer ranges will be acceptable for creating Pickering emulsions (Aveyard *et al.*, 2003). Adsorption and desorption of solid particles at the emulsion interface are reversible processes (Hirose *et al.*, 2008). However, nanoparticle adsorption is irreversible since the energy required for nanoparticle desorption exceeds thermal energy. Meanwhile, the surface energy reduction of droplets drives nanoparticle adsorption on emulsion droplets. This is a thermodynamic phenomenon. As a result, various NPs, particularly IONPs, has recently been employed to stabilise Pickering emulsions.

2.1.1 Pickering emulsion stabilisation

Figure 2.2 shows that the typical emulsion system is thermodynamically unstable and readily degrades since there are no molecule adsorptions for stability (Roohinejad *et*

al., 2018a). The high free energy of nanoparticle desorption may lead to irreversible nanoparticle adsorption at the O/W interface (Roohinejad *et al.*, 2018b). The emulsion will have a strong energy barrier allowing the thermodynamically unstable emulsion to be stabilised (Aveyard *et al.*, 2003).

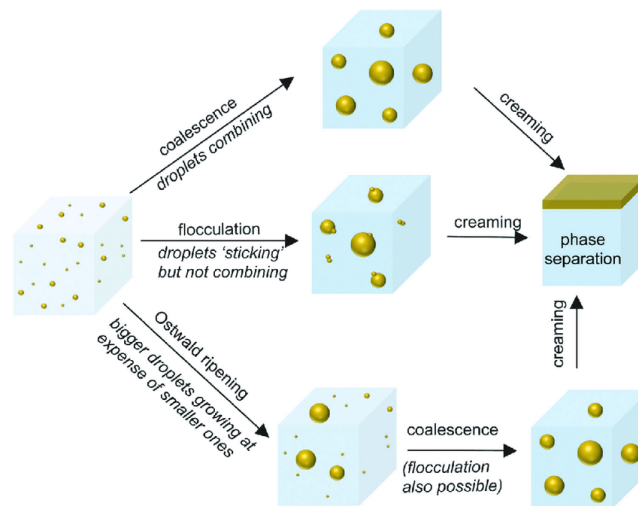


Figure 2.2: Schematic diagrams represent the different destabilisation mechanisms of O/W emulsion (Gupta *et al.*, 2016).

Figure 2.2 depicts two situations contributing to the emulsion's structural alterations, mainly caused by flocculation or coalescence. In flocculation, droplets approach one another due to attractive interactions and move as a unit. In contrast, droplets combine during coalescence to form a larger droplet (Gupta *et al.*, 2016). Coalescence is the flocculation mechanism that occurs once the van der Waals force becomes strong.

To avoid coalescence, surfactant molecules were added to the emulsion to minimise interfacial tension (Leong *et al.*, 2015). To get high desorption energy, the wettability of NPs must increase, as in Pickering emulsions; this will prevent NPs from separating from the O/W interface. Because most NPs are hydrophilic, the nanoparticle

is coated with organic matter to change its wettability. For instance, iron oxide nanoparticles (IONP) containing PSS may enhance nanoparticle adsorption at the oil-water interface by interacting hydrophobically with the oil phase during emulsion stabilisation (Tham *et al.*, 2021).

The second point of view is based on the overall colloidal stability of the Pickering emulsion. Pickering colloidal stability depends on emulsion droplet flocculation until the creaming phase. The interaction forces between the emulsions highly impact the emulsion flocculation (Gupta *et al.*, 2016). Polyelectrolyte PSS-coated NPs may influence the steric and electrostatic forces' short-distance repulsion of the Pickering emulsion against the van der Waals forces to improve the colloidal stability of emulsion droplets (Tang *et al.*, 2015)

Surfactants might minimise the interfacial tension at the O/W contact. At the same time, NPs with high desorption energy could keep the emulsion from coalescing (Binks *et al.*, 2007). The negative charge of silica NPs allows cationic surfactants, which have the opposite charge, to stick to them. This makes the surface of the NPs less hydrophobic, stabilising the emulsion. Also, the size of the Pickering emulsion decreased as the surfactant concentration rose. However, synergistic stabilisations the competition for adsorption between solid NPs and surfactants at the O/W interface (Aveyard *et al.*, 2003).

2.1.2 Stimuli-responsive and potential application of Pickering emulsion

As previously stated, the organic matter surface coating on NPs provides steric and electrostatic force. Two major external environmental elements influence electrostatic and steric forces. pH and ionic strength are the two environmental parameters. The pH and ionic strength of the emulsifier might modify its organic matter

conformation and, as a result, the responsiveness of the emulsion (Xiao *et al.*, 2018). Tham *et al.* created a magnetic Pickering emulsion (MPE) through IONP stabilised by PSS and CTAB (Tham *et al.*, 2021). On a macroscopic scale, the magnetic separation efficiency of MPE reached 90% at all pH ranges. However, MPE's colloidal stability was lowest at pH 10 compared to pH 3 and DI water conditions. MPE at pH 10 experiences irreversible flocculation during magnetophoresis.

Aside from pH and ionic strength, several external factors cause different Pickering emulsion responses (Pang, Laplante and Filkins, 2012). These responses have arisen due to the chemical or physical features of coating materials or NPs. Ionic surfactants such as SDS and CTAB are usually used. Yuan and He studied the effect of poly (diallyl dimethylammonium) chloride (PDDA) as a surfactant for aurum NPs (AuNPs). Their findings indicate that positively charged PDDA-AuNPs with a low optimal concentration might considerably improve polymerase chain reaction (PCR) specificity and efficiency (Yuan and He, 2013).

Utilization of IONPs is on the rise due to their inherent low toxicity and magnetic properties, making nanoparticle separation from fluids simple. Nanoparticles have recently been evaluated for oil removal from bodies of water. MPE absorbs oil quite selectively, for instance (Tham *et al.*, 2021). One of the most notable advantages of this MNP-based water treatment technique is the ability of MNPs to recall, which may be easily achieved by using a hand-held permanent magnet once the hazardous component has been adsorbed onto the particle surfaces (Lim *et al.*, 2014a).

2.2 Iron oxide nanoparticles (IONP)

Iron oxides are a class of chemical compounds that exist in various polymorphic forms, including γ -Fe₂O₃ (maghemite), Fe₃O₄ (magnetite), and FeO (wustite) (Ajinkya *et al.*, 2020). Magnetite, maghemite, and hematite are the three most frequent types of iron oxide. Hematite has the lowest magnetism of the three iron oxides, while magnetite has the greatest magnetisation (Dar and Shivashankar, 2014). As a result, magnetite is the most popular material for use as a magnetic carrier in engineering applications. Maghemite and magnetite are the most explored since they exhibit unique features at the nanoscale because quantum effects impact both matter behaviour and optical, electrical, and magnetic properties. The quantum effect dominates the behaviour of IONP in the nanoscale range, affecting the matter's magnetic, electrical, and optical characteristics. At the nanoscale, individual atoms or molecules that influence the feature are assigned to the sum of all the quantum forces affecting all the atoms at the bulk size. For instance, superparamagnetic IONPs smaller than 20 nm are magnetic (Ajinkya *et al.*, 2020).

Compared to the majority of mineral oxide NPs, the distinctive attribute of IONP is its superparamagnetic property. When there is no magnetic field, superparamagnetic IONPs has zero magnetisation. IONPs, on the other hand, can exhibit high magnetisation saturation in the presence of a magnetic field (Faraudo and Camacho, 2010). Due to their nanoscale size and large surface area, NPs have unique physical and chemical characteristics (Khan *et al.*, 2019). IONP is frequently employed in engineering applications due to its unique magnetic characteristic and big surface area – namely, Magnetic Resonance Imaging (MRI) and oil recovery (Tham *et al.*, 2021).

Co-precipitation is often the most practical and straightforward chemical approach for preparing IONP from salts' aqueous solution under alkaline pH. IONP has cheap costs, low energy requirements, and excellent products for both research and

industrial applications (Zhu and Wu, 1999). Since IONP generated by co-precipitation has a wide size range in nanometers, numerous changes have been made to restrict the IONP cluster size (Zhu *et al.*, 2018).

2.2.1 Stabilisation and surface functionalisation of naked IONP

Due to their nano-size, IONP has a high ratio of surface area to volume (Khan *et al.*, 2019). Naked IONP with low colloidal stability is unsuitable for research and engineering applications. Hence, numerous ways for enhancing the colloidal stability of IONP are discussed.

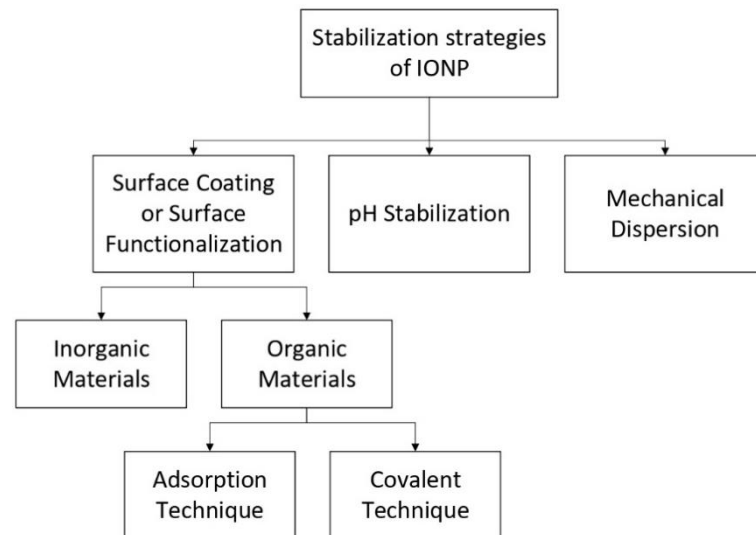


Figure 2.3: Stabilisation strategies reviewed for the naked IONP (Tham *et al.*, 2021).

Three main methods are employed for stabilising IONP in research and engineering applications, as indicated in Figure 2.3. Surface coating, pH stabilisation and mechanical dispersion by ultrasonication are a few methods to stabilise naked IONP (Tham *et al.*, 2021). Ultrasonication and pH stabilisation are two easy ways to improve its colloidal stability. Yang *et al.* discovered that ultrasonication of IONP for 10 minutes yields nano-size particles (2005).

pH stabilisation also can improve IONP colloidal stability. Tham and co-workers discovered that severe acidic or alkaline pH could further diminish the average sizes of IONP formed by co-precipitation (Tham et al., 2021). Lastly, the surface coating prevents naked IONP from quickly oxidising in air and losing its magnetism (Laurent et al., 2008). The hydroxyl group of IONP will be protected by a coating on the surface of IONP, which will delay the oxidation process (Wu *et al.*, 2015).

Nevertheless, surface coating is the most widely-used approach for IONP stabilisation. The exterior shell of IONP is made of two different materials – organic molecules and inorganic NPs. A reducing agent can coat inorganic NPs, such as gold NPs, onto the core magnetic core of IONP (Yang et al., 2014). However, since gold and silver are expensive noble metals, they cannot be used for water purification. Furthermore, most inorganic NPs are classified as heavy metals, causing heavy metal contamination in the environment.

Compared to the inorganic shell of IONP, organic molecules are the preferred surface coating material because they are both eco-friendly and biocompatible. The IONP surface coating was divided into two major techniques: adsorption and covalent (Biehl *et al.*, 2018). Before grafting long-chain polymers onto the NP's surface, the covalent method requires NPs contain their functional group. The polymer grafted onto the IONP will induce steric repulsion between NPs.

Conversely, the adsorption method will be simpler than covalent techniques. The adsorption process is driven by electrostatic attraction between adsorbed organic molecules (polyelectrolytes) and NPs (Toh *et al.*, 2012). It calls for fewer surface modification techniques and anionic or cationic molecules deposition on the NPs. On the surface of IONP, polyelectrolytes produce electrostatic and steric repulsion between NPs (Tham *et al.*, 2021).

The surface coating of IONP with organic and inorganic compounds is a stabilising method that can help functionalised the IONP, especially for engineering applications. Similar to this research, the polyelectrolyte PSS adsorbing on the IONP could be assembled by an additional layer of PDDA (Wong *et al.*, 2008). Adsorption of polyelectrolytes on NPs surfaces via charge neutralisation and charge resaturation resulted in charge reversal on the material surface and the layer-by-layer polyelectrolyte assembly on the NP's surface (Ariga *et al.*, 2011; Berndt *et al.*, 1992).

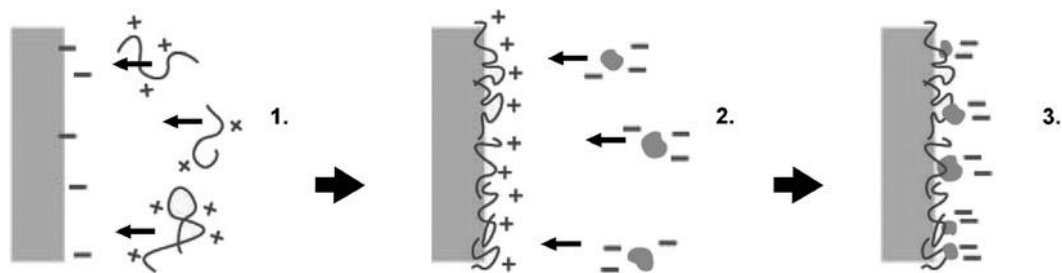


Figure 2.4: Illustration shows a layer-by-layer polyelectrolyte approach where adsorption of charged materials to oppositely charged surfaces (McShane and Lvov, 2014).

In addition, polyelectrolyte-coated NPs nowadays are used to form complexation with surfactant molecules (Chiappisi *et al.*, 2013). In general, the complexation of polyelectrolyte and surfactants is influenced by the features of polyelectrolyte-coated NPs, notably surfactant and polyelectrolyte concentration, polyelectrolyte molecular weight, polyelectrolyte stiffness, and polyelectrolyte charge density (Chiappisi *et al.*, 2013) For instance, raising the concentration of the surfactant would alter the structure of the polyelectrolyte by inducing micelle formation during the interaction between the polyelectrolyte and the surfactant (Fundin and Brown, 1994)

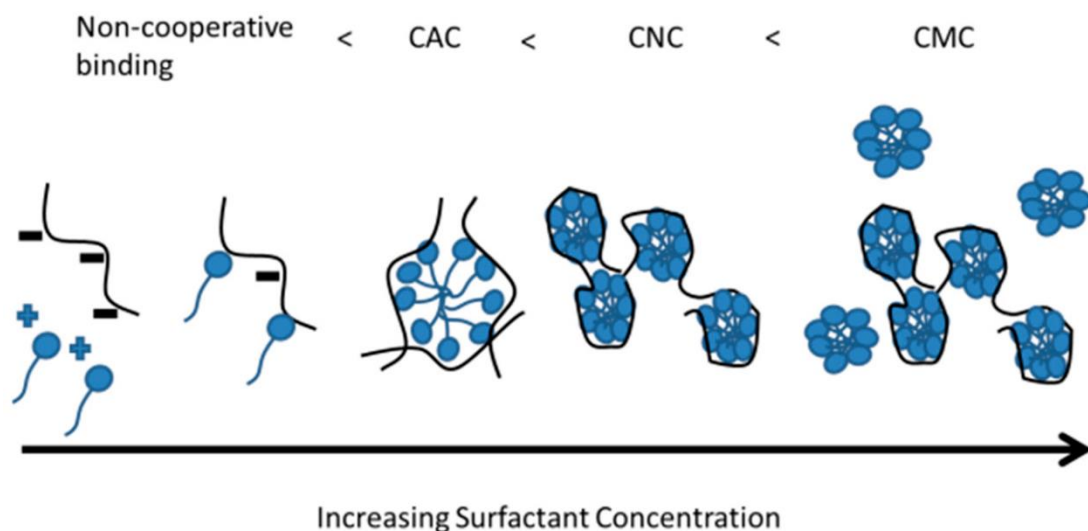


Figure 2.5: Illustration of the evolution of the micelle-like structure of surfactants on polyelectrolyte as surfactant concentration increases (Khan and Brettmann, 2018).

2.2.2 IONP and IONP-composites colloidal stability

Colloidal stability, including dispersion and aggregation of NPs, constituted a barrier to manipulating NPs in engineering applications. The collision frequency and collision efficiency of IONP largely determine the colloidal stability (Champagne *et al.*, 2018; Tham *et al.*, 2021). The primary factor influencing the collision frequency of IONP is Brownian motion. Meanwhile, IONP collision efficiency is determined by particle contact forces such as van der Waals, electrostatic, steric, magnetic, and hydration (Tham *et al.*, 2021).

Brownian motion of IONP is caused by the random movement of IONP in a fluid, which might result in IONP collisions. The diffusion coefficient of IONP, D_t , may be represented using the Stoke-Einstein equation as follows:

$$D_t = \frac{k_B T}{3\pi\eta d_h} \quad (2.2)$$

Where k_B represents the Boltzmann constant, T represents the absolute temperature, η represents the suspension viscosity, and d_h represents the IONP hydrodynamic diameter (Tham *et al.*, 2021).

IONP diffusivity is influenced by the size, viscosity, and temperature, according to the equation. When IONP diameters are reduced to less than 100 nm, IONP diffusion rises, and IONP collisions become more frequent. The smaller the IONPs hydrodynamic diameters, the quicker their aggregation rate. The particle collision frequency, Z_{AB} , is determined as follows (Chai *et al.*, 2015):

$$Z_{AB} = n_A n_B (r_A + r_B)^2 \sqrt{\frac{8\pi k_B T}{\mu_{AB}}} \quad (2.3)$$

Where n_A and n_B represent the number densities of species A and B , r_A and r_B represent the hydrodynamic radii of the species, k_B represents the Boltzmann constant, and μ_{AB} represents the reduced mass of both species (Chai *et al.*, 2015).

The concentration of IONP, which promotes aggregation by raising the probability of collisions, is one of the experimental variables that may influence the collision frequency, as shown by the equation above (He *et al.*, 2008). Steric and electrostatic forces are repulsive interactions between NPs that increase colloidal suspension stability (Champagne *et al.*, 2018). As the natural substance of NPs is governed as IONP, it always happens depending on the radius and distance between NPs. IONP's outcome, whether aggregated or scattered, is determined by balancing the

electrostatic force, steric force, and van der Waals force. Surface coating is the most fundamental method for boosting steric and electrostatic force (Tham *et al.*, 2021).

2.3 Magnetic separation

Magnetic separation is a method that utilises an external magnetic field to remove molecules with magnetic properties. Magnetic materials, on the other hand, have varying magnetic susceptibilities, necessitating a distinct modification of the magnetic field to separate the materials. Different levels of magnetic field strength/gradient can be used to differentiate ferromagnetic and paramagnetic materials (Ellis, 1999). To separate weakly paramagnetic materials in suspension, a high gradient magnetic separation (HGMS) process was developed using a matrix of stainless steel wool with a high magnetic field gradient ($\sim 10^6$ T/m) as the packing material in the separation column. HGMS is a continuous flow method that separates magnetised particles from a liquid mixture using a high magnetic field gradient ($\nabla B \geq 100$ T/m) that can be created only by an electromagnet supplied with intensive electrical power (Mooser *et al.*, 2004). Using an external magnetic field, nano-sized and micro-sized particles are magnetically separated instantaneously (Ellis, 1999; Tham *et al.*, 2021). After HGMS, the packing was demagnetised by removing the magnetic field, and compressed air was used to cleanse the matrix of magnetic components. HGMS is frequently used in mineral processing, water treatment, and the purification of cells and proteins (Ge *et al.*, 2017).

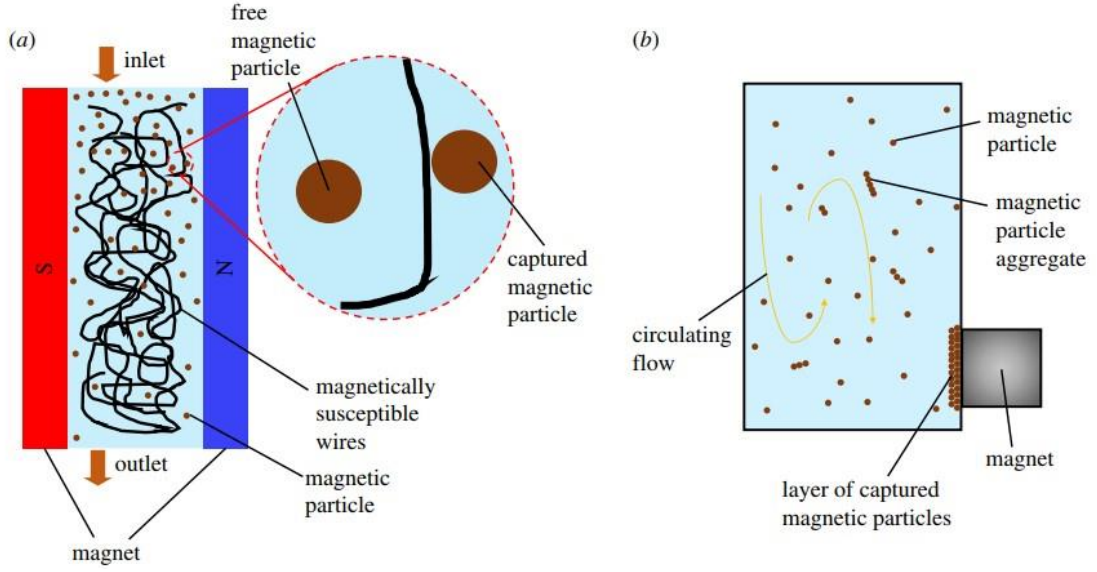


Figure 2.6: HGMS and LGMS processes (Leong *et al.*, 2016a).

As in Figure 2.6(a), an HGMS column is composed of a magnetisable coiled wire in the centre of the magnetic separation column. This wire coil introduces disturbances into the magnetic field, resulting in a much stronger and more localised magnetic field gradient on the wire coil (Hatch and Stelter, 2001). Since the magnetophoretic attraction force experienced by a magnetic particle is precisely proportional to the magnetic field gradient, the magnetic particle encounters a tremendous magnetophoretic force as it passes through the region near the magnetisable wire (Leong *et al.*, 2016a; Tham *et al.*, 2021):

$$F_m = \frac{4}{3}\pi r^3 \mu_o M \nabla H \quad (2.3)$$

Where F_m represents the magnetophoretic force exerted on a single magnetic particle, r represents the radius of the magnetic particle, μ_o is the permeability of free

space, M is the volumetric magnetisation of magnetic particle, and ∇H is the magnetic field gradient.

However, there are significant downsides to using the HGMS approach for MNP separation. First, a massive quantity of electric energy is required to operate the electromagnet, resulting in a hefty utility cost (Toh *et al.*, 2012). Additionally, the HGMS approach has some disadvantages, including a high capital cost, the complexity of establishing an analytical solution to characterise the transport behaviour of MNP in the column, and severe MNP deposition on the wire coil, which is difficult to clean (Leong *et al.*, 2016b).

To address the shortcomings of HGMS, as mentioned earlier, low gradient magnetic separation (LGMS) has become widely used to separate weak paramagnetic materials due to the magnetic field of less than 100 T/m (Lim *et al.*, 2011a). This significantly simplifies the magnetic separator's internal construction (de Las Cuevas *et al.*, 2008a). It shows excellent efficiency in batchwise separation techniques conducted at the laboratory scale (Benelmekki *et al.*, 2011). LGMS's remarkable separation efficiency is attributed to the MNPs' self-aggregation property in the presence of an external magnetic field, which is not considered in standard magnetophoresis theory (Yavuz *et al.*, 2006).

Figure 2.6(b) shows that a permanent magnet generates a magnetic field gradient over the to-be-separated magnetic particle solution. Therefore, magnetic particles are separated from the solution by migrating to the region with the strongest magnetic field gradient near the magnet. Both particle aggregation and continuous circulating flow occur throughout the process, leading to the distortion of the magnetophoretic path of MPs (Leong *et al.*, 2016a). MNPs get magnetised when exposed to an external magnetic field, gain a net magnetic dipole moment, and migrate toward the magnetic source. MNPs clash

during migration to form larger aggregates because, in the MNP solution, they act like small magnets due to their magnetic dipole (Leong *et al.*, 2016a). When MNPs aggregate into larger aggregates, the enhanced magnetophoretic force works on the particle clusters to overcome opposing forces such as viscous drag and thermal fluctuation, thus separating them within an acceptable timeframe (Andreu *et al.*, 2011).

Due to the nonhomogeneity of the magnetic field throughout the magnetic particle solution, magnetophoretic motion begins. The magnetic particles migrate to the region with the greatest magnetic field gradient (Lim *et al.*, 2011b). Magnetic particles are removed from the suspending medium, and the separation is completed. Since the magnetic field strength decreases rapidly with distance from the magnet, the magnetic field gradient across the entire volume of magnetic particle solution subjected to separation is typically less than 100 Tm^{-21} (Leong *et al.*, 2015).

Nonetheless, one significant limitation of LGMS is its small magnetophoretic force met by the magnetic particles to be separated due to the LGMS (Lim *et al.*, 2014b). Two forces work against deterministic magnetophoretic movement of magnetic particles: viscous drag and thermal motion. Viscous drag, F_{drag} is occurred by friction during the motion of particles relative to the surrounding fluid. The Stokes equation may be used to determine the amount of viscous drag:

$$F_d = 6\pi\eta r v \quad (2.4)$$

Where F_d is the viscous drag experienced by the magnetic particle, η is the viscosity of the suspending fluid, and v is the MP's magnetophoretic velocity relative to the fluid (Leong *et al.*, 2015). The value of the diffusion coefficient D of a particular particle in suspension may be used to determine the degree of thermal fluctuation, as indicated by the Stokes-Einstein equation in (5) (Leong *et al.*, 2016a). Magnetophoretic

force F_m varies directly proportional to r^3 according to the F_m and Stokes equations, but opposing viscous drag F_d is proportional to r .

Due to the small size of the magnetic particle, r and viscous drag dominate the magnetophoretic force, forcing magnetic particles to migrate slowly toward the magnet pole. This will result in the effective completion of the separation. Due to the magnetic particle's small size, its thermal fluctuation is more pronounced. This randomisation of magnetic particles' magnetophoretic paths makes it difficult to control their velocity. Reynolds number (Re) and Peclet number (Pe) are significant dimensionless numbers that characterise, respectively, the ratio of inertia force from magnetophoretic to viscous drag force and diffusive force (Lim *et al.*, 2014b). According to this dimensionless analysis, magnetophoretic force dominates viscous drag and diffusion in determining the motion of magnetic nanoparticles when Re and Pe are greater than unity. As a result, these requirements must be met before developing a more detailed design for the specific LGMS process.

Numerous applications utilise LGMS. Chong *et al.* developed a mathematical model to represent the kinetic of continuous flow LGMS (CF-LGMS) utilising PDDA-coated MNPs with a diameter of 64.4 nm and hydrodynamic diameter of 107 nm. This model determined the influence of essential design factors on separation efficiency. From their simulation results, CF-LGMS separation performed under low MNP solution flowrate and high particle concentration yielded a 98% separation efficiency (Chong *et al.*, 2021). Some additional mathematical models explored the dynamic behaviours of superparamagnetic IONPs in an LGMS (Zhu *et al.*, 2018). Other notable LGMS applications include heavy metal (Yavuz *et al.*, 2006), the removal of microalgae (Toh *et al.*, 2012) and biomedical cell separation (Zborowski *et al.*, 2003).

The separation of MPE under LGMS involves two levels of detail: the microscopic motion of individual emulsions and the macroscopic separation kinetics resulting from their collective motion. This report will focus solely on macroscopic motion to fulfil the research objectives.

CHAPTER 3

METHODOLOGY

3.1 Research flow

Figure 3.1 is the flow diagram for the research project on oil-from-water removal under a low gradient magnetic separation (LGMS). Preparation of MPE was carried out in the nanoparticle research laboratory in USM. After the oil-to-water ratio range for LGMS was determined, data was collected, and the collected data were analysed. After all of the data required for this research was collected, report writing was done.

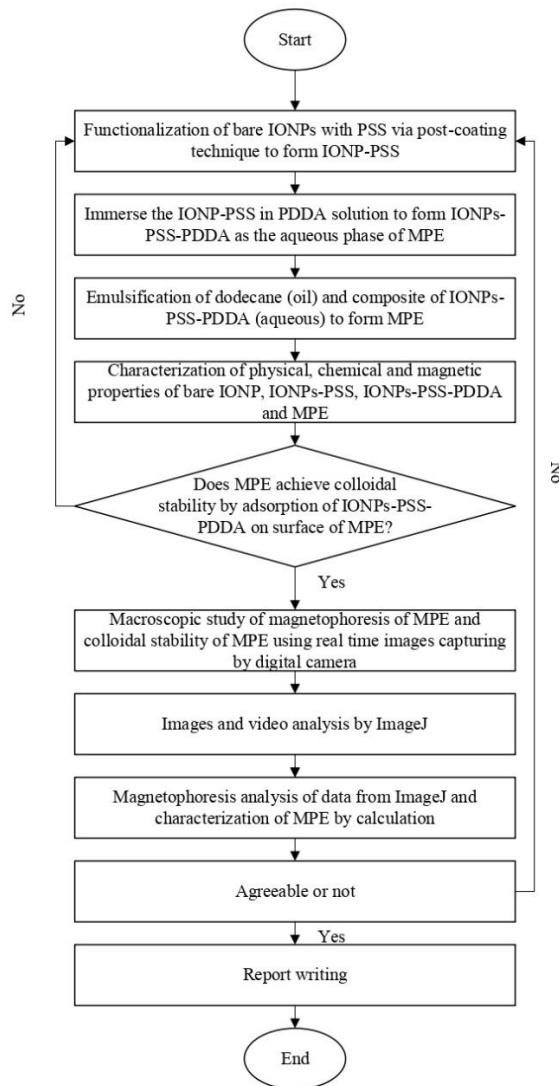


Figure 3.1: Flow diagram on a research project for oil-from-water removal under LGMS.

3.2 Materials

In this project, naked Iron Oxide Nanoparticles (Fe_3O_4) $\geq 99\%$ are from SkySpring NanoMaterials, Inc. For naked IONP coating, sodium sulfonated polystyrene (PSS) powder (70,000 g/mol) is used. Poly(diallyldimethylammonium chloride) (PDDA) with a medium molecular weight (200,000–350,000 g/mol). The Elga Purela produces the deionized water required for the project. A 7mm-diameter, 15mm-tall cylindrical grade N50 neodymium ferrite boron (NdFeB) magnet was acquired for the macroscopic study on the MPE separation.

Table 3.1: Materials used, supplier and purpose

Material	Supplier	Purpose
IONP	SkySpring NanoMaterials, Inc	The base nanoparticle itself
PSS	Sigma Aldrich Pte. Ltd.	Functionalize IONP via post-coating
PDDA	Sigma Aldrich Pte. Ltd.	Functionalize IONP via post-coating
Dodecane	Sigma Aldrich Pte. Ltd.	Organic solvent for emulsifying IONP-composite to become MPE
NdFeB magnet	Ningbo Yuxiang	Macroscopic study of MPE separation
NaOH	Fisher Scientific Pte. Ltd.	pH correction
HCl	Fisher Scientific Pte. Ltd.	pH correction

3.3 Functionalization of IONP

The approach for surface functionalized by PSS via post-coating technique is detailed in this section. Functionalized IONP may improve IONP colloidal stability and avoid irreversible aggregation.